Static gravity field modelling using the GOCE hl-SST data in individual accelerometer mode

Zou Xiancai

School of geodesy and geomatics, WHU

The 2nd DAAD TN workshop

24-28 July, 2018, Luxembourg

Background

hl-SST and Centre of Mass Trimming

- Motion of a particle (don't distinguish b.w. A&F)

$$\vec{a} = \vec{f} + \nabla V - \ddot{\vec{b}} - 2\vec{\omega} \times \vec{v} - \vec{\omega} \times \left(\vec{\omega} \times \vec{r} \right) - \frac{d\vec{\omega}}{dt} \times \vec{r}$$

- Proof mass of accelerometer

$$\vec{f} = \ddot{\vec{b}} - \nabla V + \vec{\omega} \times \left(\vec{\omega} \times \vec{r} \right) + \frac{d\vec{\omega}}{dt} \times \vec{r}$$

- Mass centre of satellite

$$\vec{f}_{CM} = \ddot{\vec{b}} - \nabla V$$

- Function of the CMT

$$\vec{f} \rightarrow \vec{f}_{CM} \left(\vec{r} \rightarrow 0 \right)$$

Background

Problem of the Common mode ACC

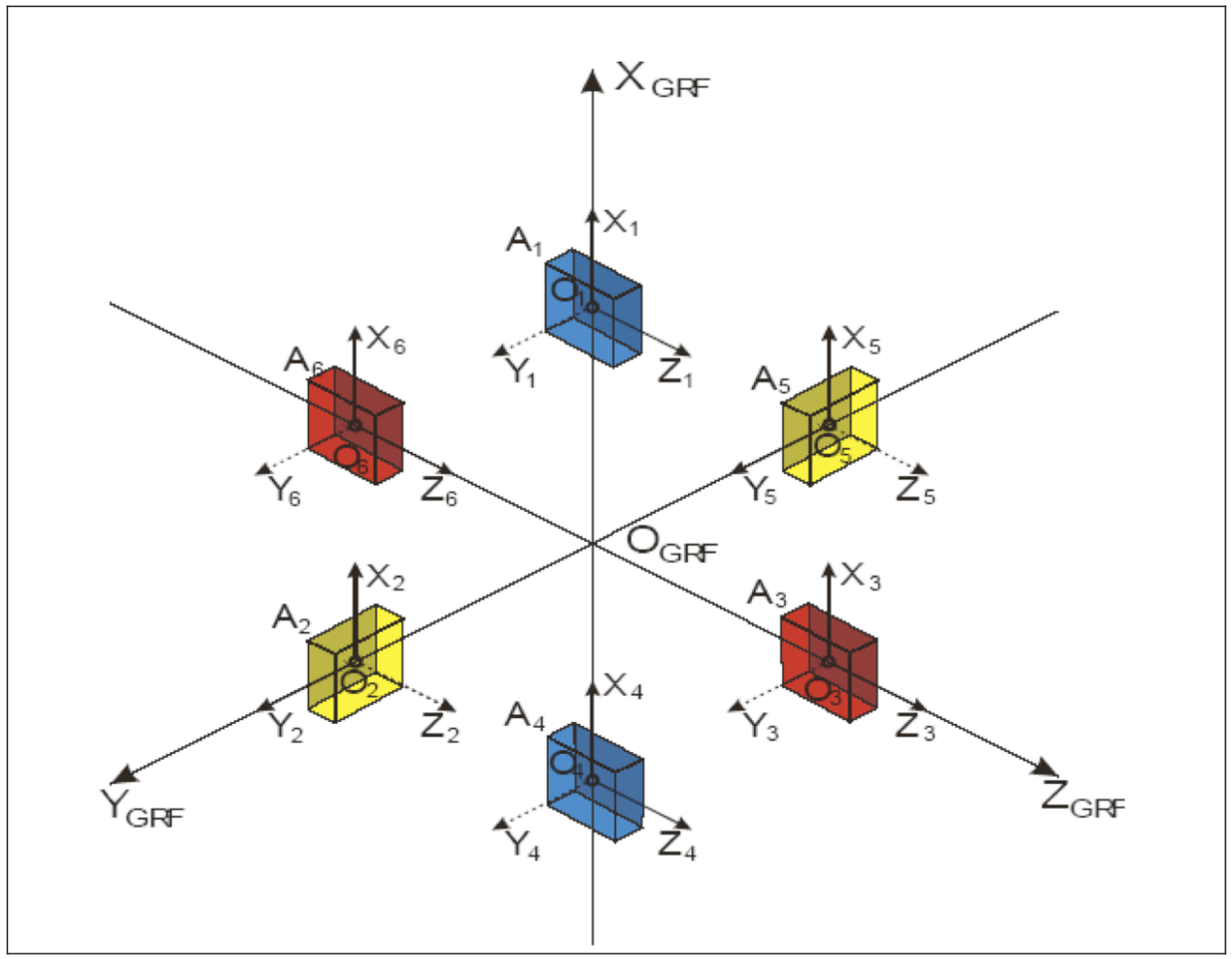

$$f_i^{CM} \equiv \frac{1}{2}\left(f_i^M + f_i^N \right)$$

$$F_i = k_i f_i^{ACC} + b_i \left(i = x, y, z \right)$$

$$\begin{aligned} F_i^{CM} &= \frac{1}{2}\left[\left(k_i^M f_i^M + b_i^M \right) + \left(k_i^N f_i^N + b_i^N \right) \right] \\ &= \frac{1}{2}\left[\left(k_i^M f_i^M + k_i^N f_i^N \right) + \left(b_i^M + b_i^N \right) \right] \end{aligned}$$

$$F_i^{CM} = k_i f_i^{CM} + b_i = \frac{1}{2}\left(k_i f_i^M + k_i f_i^N \right) + b_i$$

Fig. 1 Configuration of gradiometer onboard GOCE（Courtesy by ESA）

Background

Basic functional model

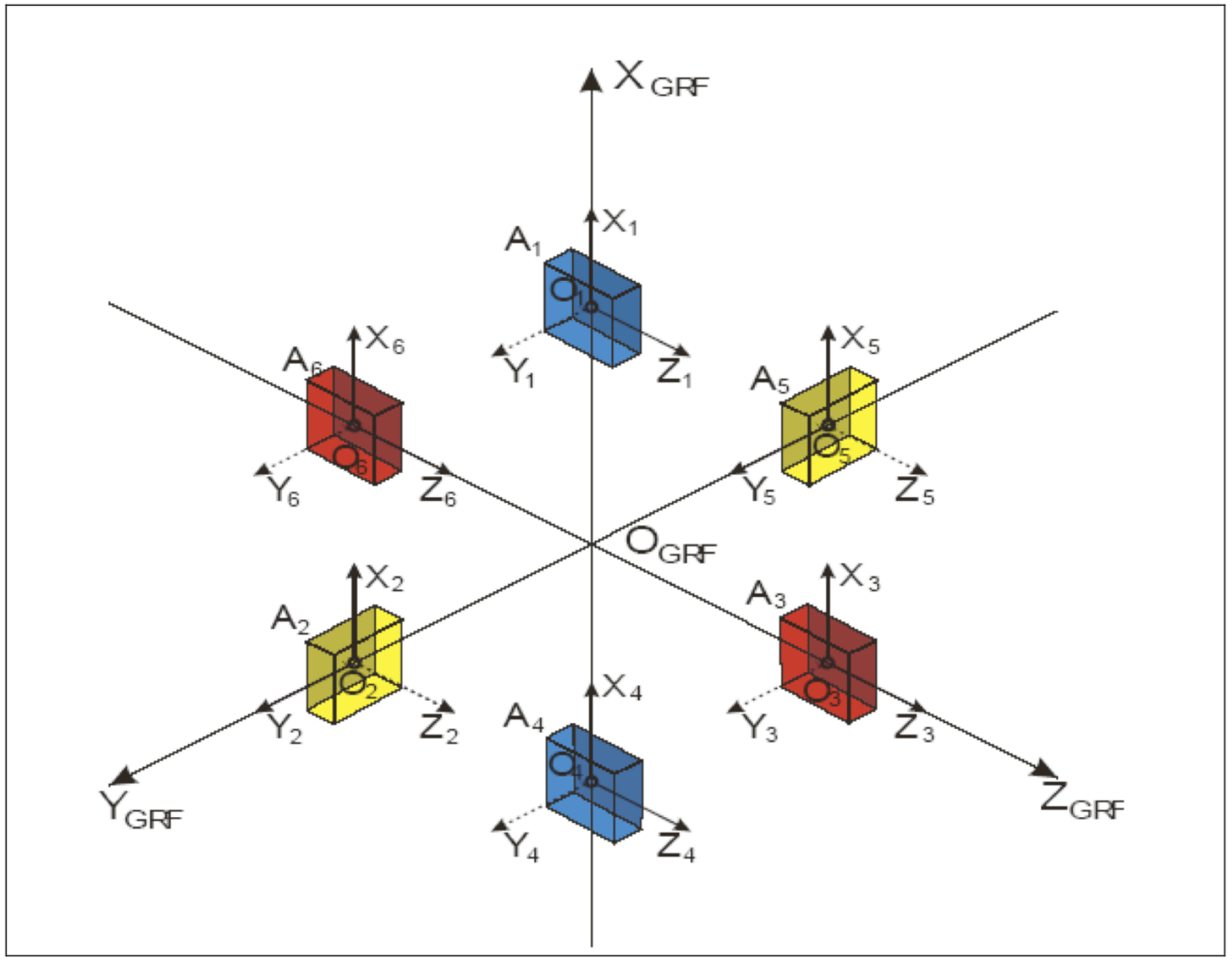

$$\mathbf{r}_{COM} = \mathrm{OI}\left(\mathbf{r}^0_{GRF}, \mathbf{v}^0_{GRF}, \nabla V_0, \mathbf{R}_{GRF\to ECI}, \mathbf{f}_i, \delta\mathbf{f}_i, \mathbf{S}_i, \mathbf{b}_i, \mathbf{r}_i\right)$$

Background

L1B GOCE data used to as a check

Tab. 1Scale factors of the six accelerometers for 11/2009

Acc No	*x*	*y*	*z*
1	1.0000	0.9914	0.9952
4	1.0000	0.9918	0.9954
2	1.0000	0.9922	0.9964
5	1.0000	0.9920	0.9973
3	1.0000	0.9915	0.9965
6	1.0000	0.9923	0.9939

Data analysing

Non-Gradational Force

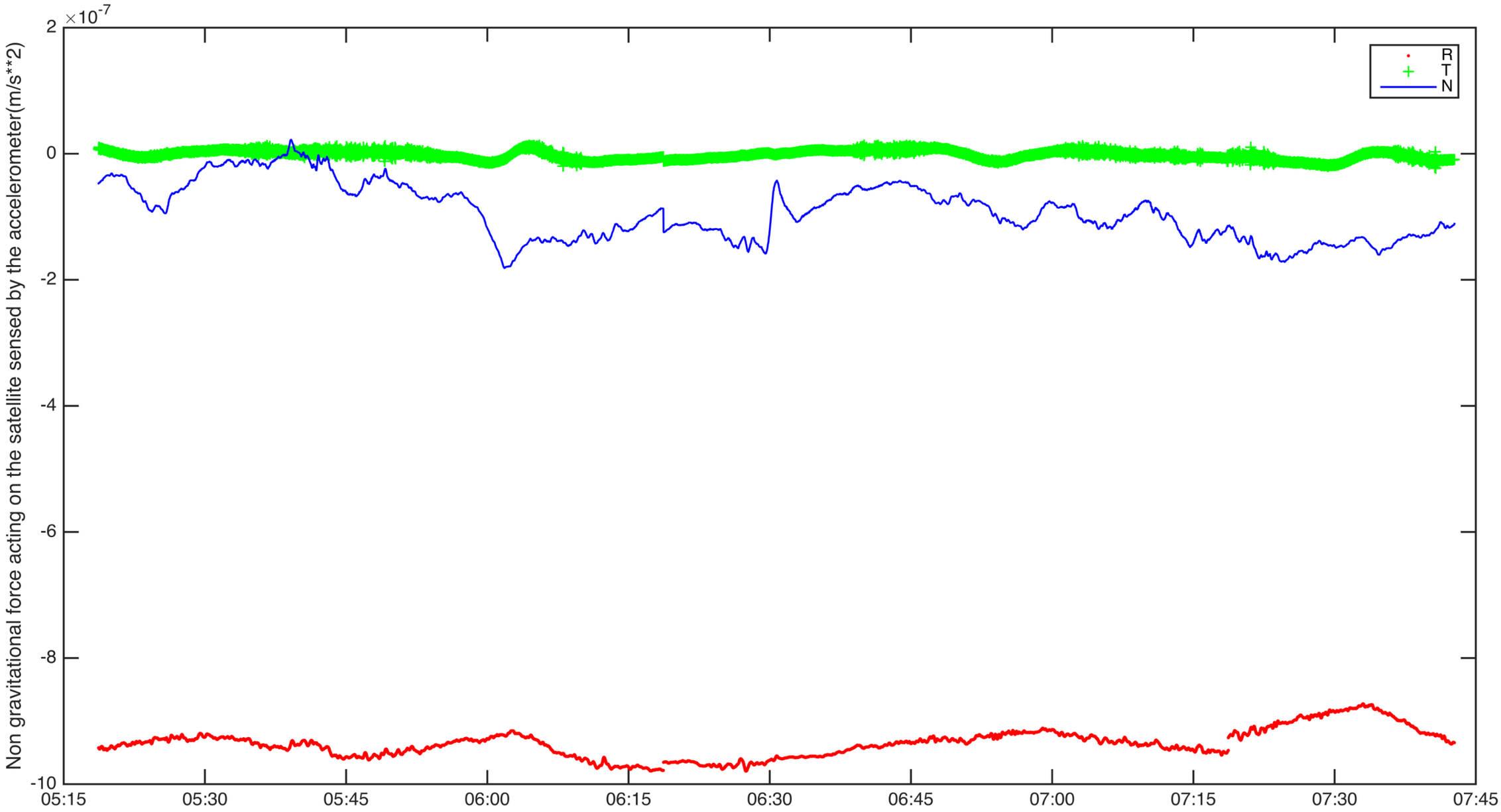

Fig. 2 Non gravitational force from the calibrated results of ACC 6. Only part of the data series is displayed as an demonstration.

Data analysing

Comparison between ACC 3 & 6, the pair on the GRF-Z axis

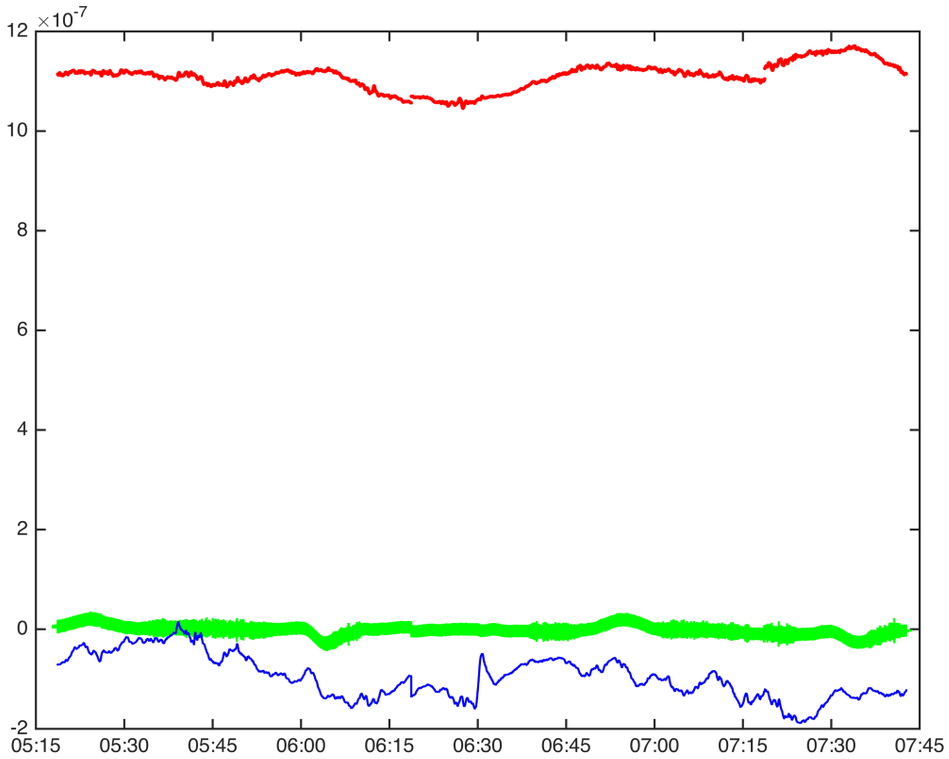

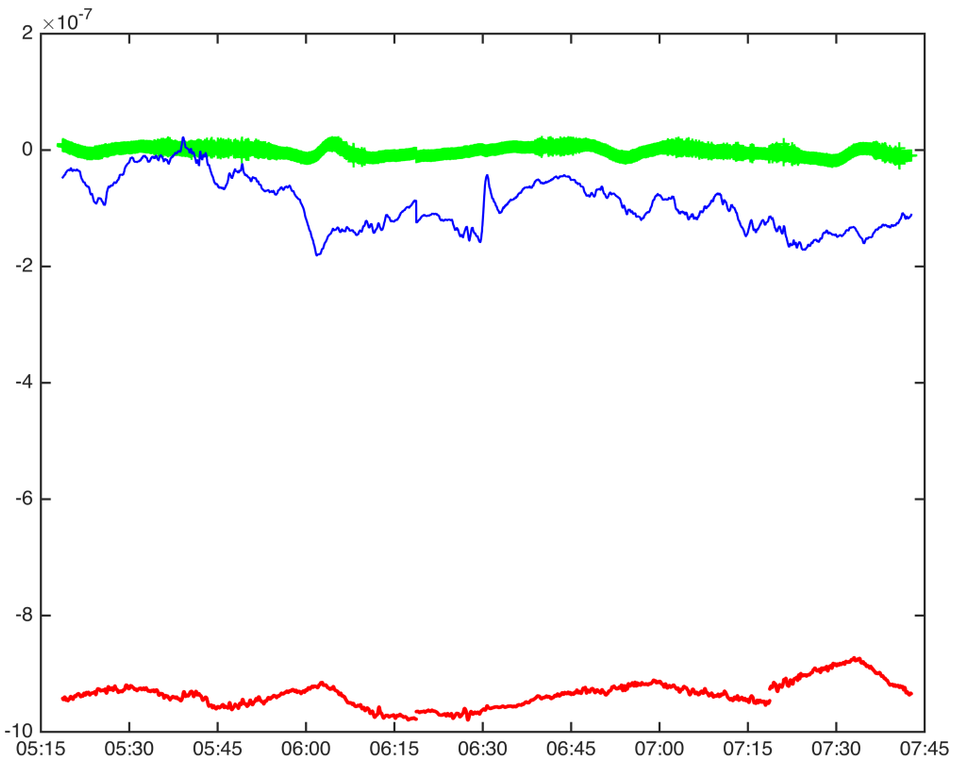

Fig. 3 NGF derived from ACC 3(left) and ACC 6 (right). Because of the mass centres are not coincided, so there exists systematic offset between these two results arising from the inertial forces.

Data analysing

NGF of the mass centre

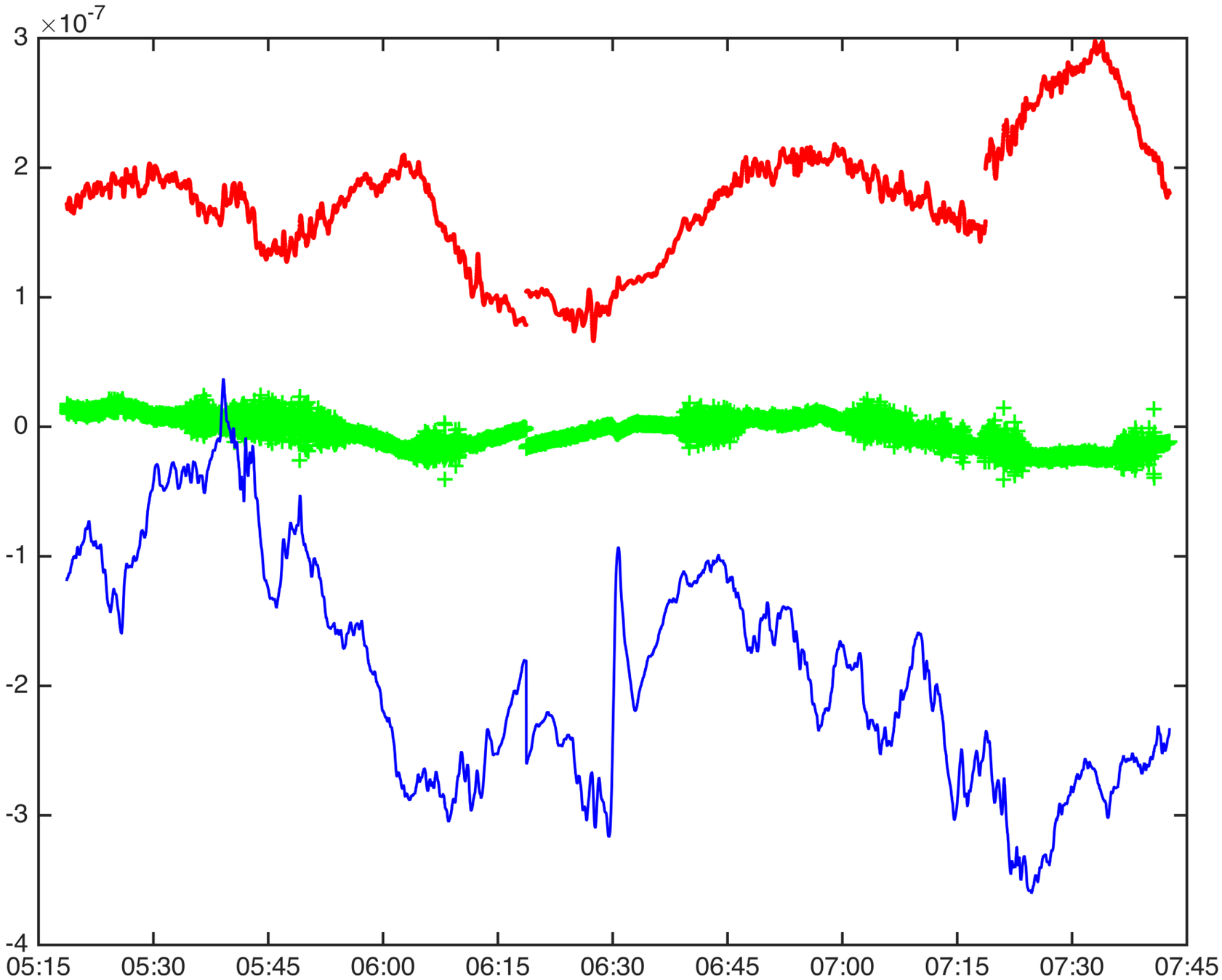

Fig. 4 NGF acting on the satellite mass centre by the summation of ACC3 and ACC6. It is the calibrated common mode acceleration.

Data analysing

ACC2 and ACC5 combination

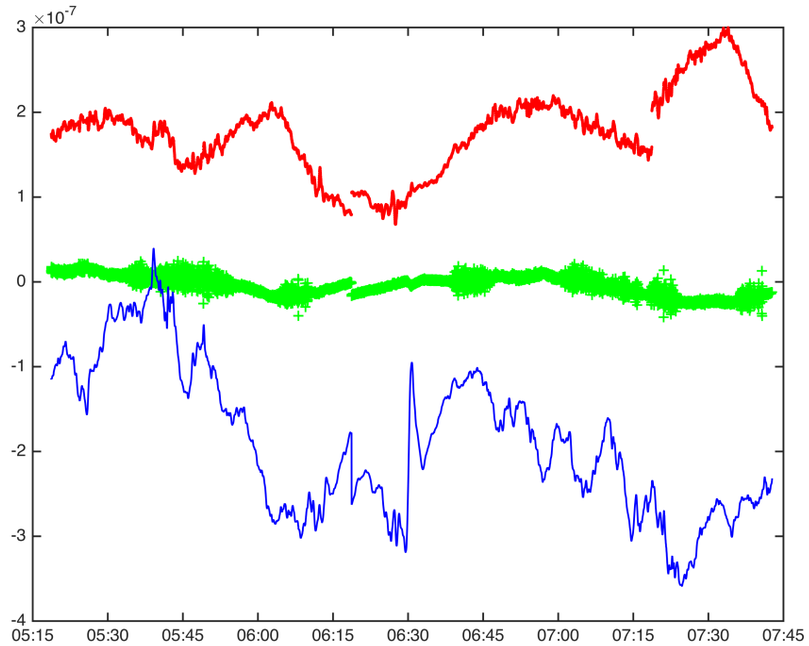

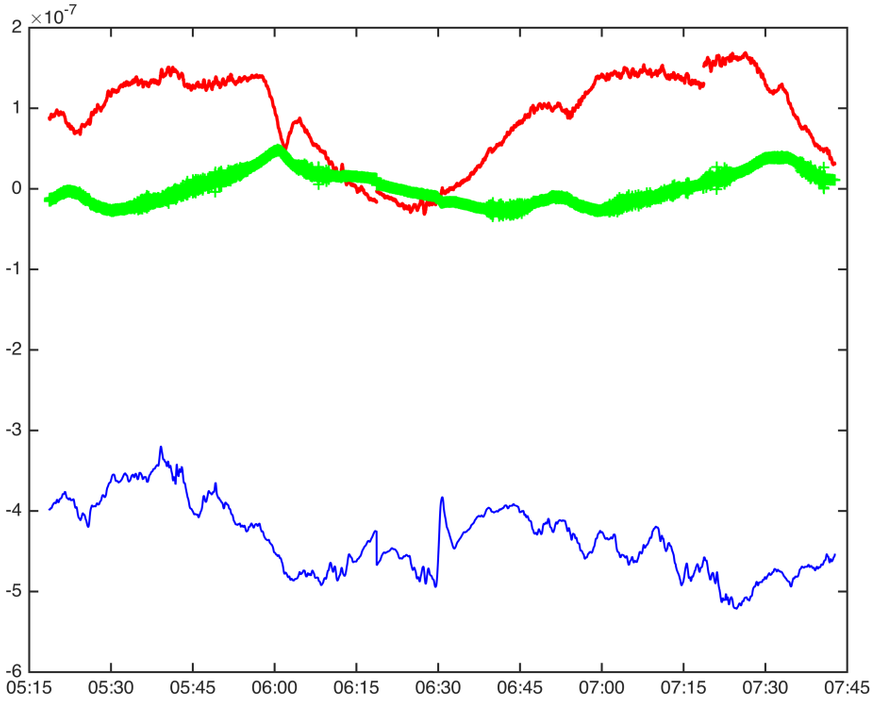

+

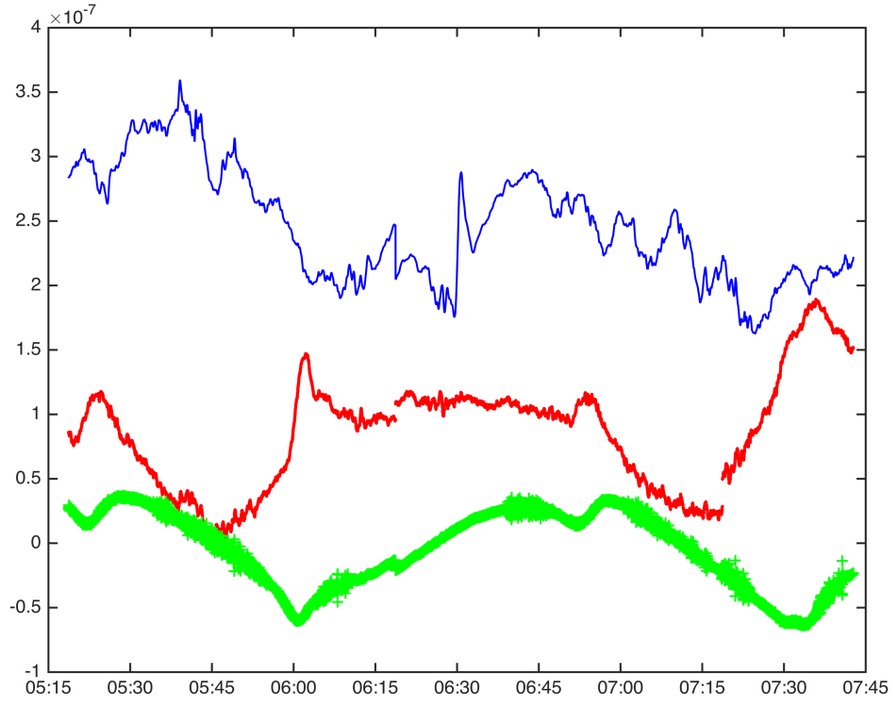

Fig. 5: Upper one is the NGF derived by the summation of ACC2 (bottom left) and ACC5 (bottom right) .

Data analysing

ACC1 and ACC4 combination

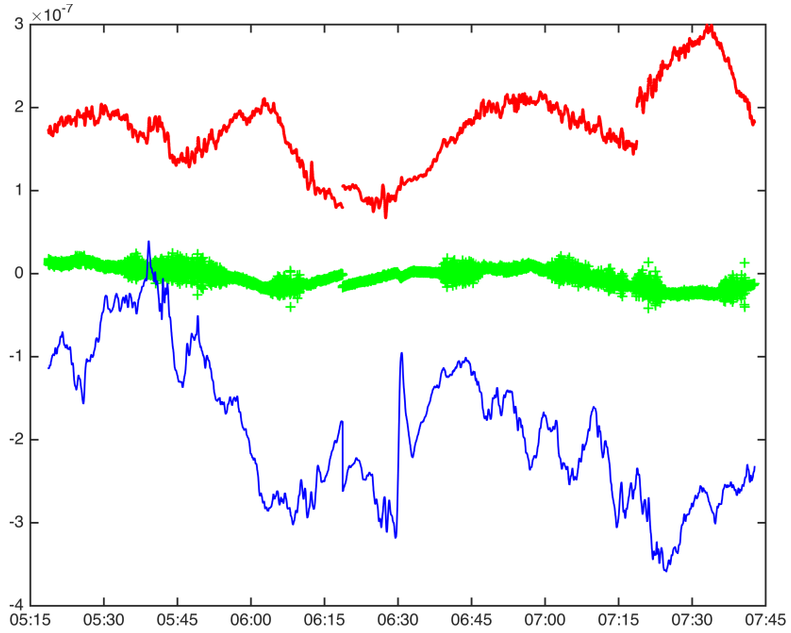

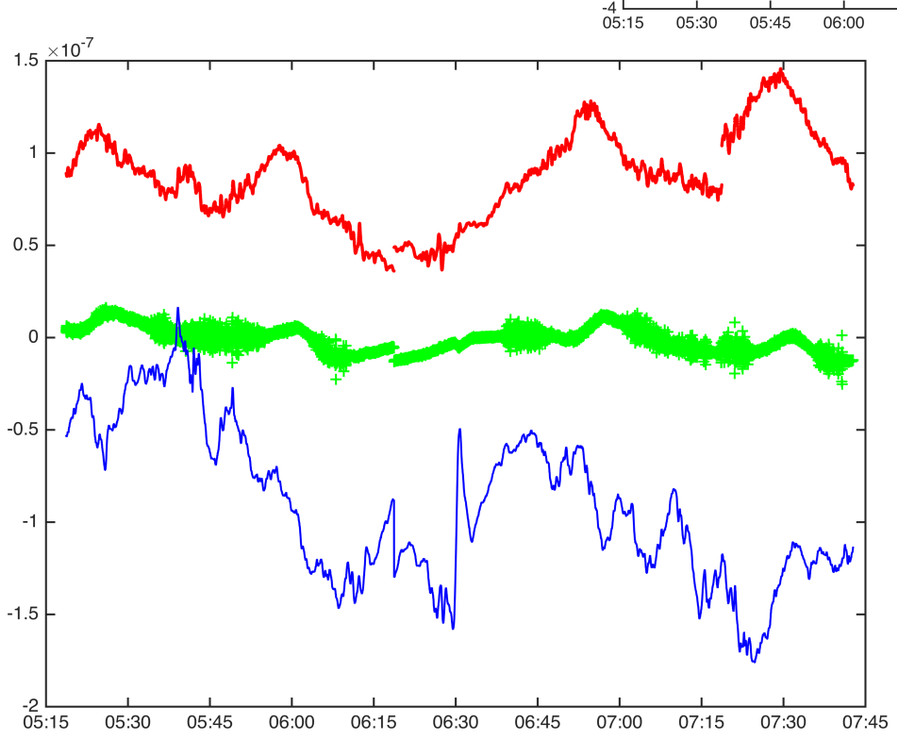

+

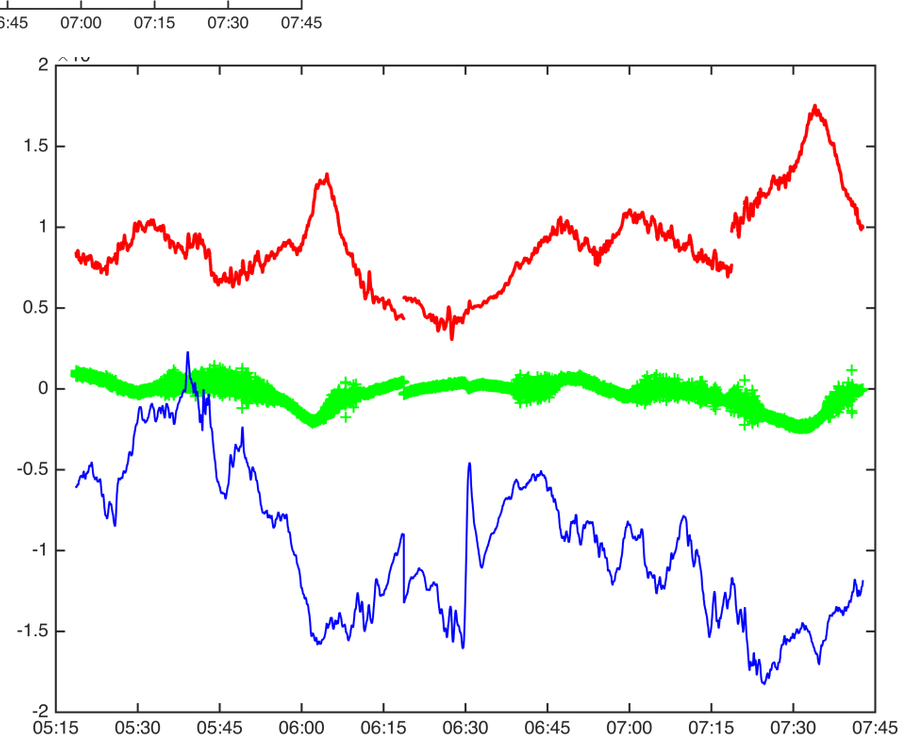

Fig. 6: Upper one is the NGF derived by the summation of ACC1 (bottom left) and ACC4 (bottom right) .

Data analysing

NGF difference between 3 pairs

Tab. 2 Difference between the 3 paris of ACC($10^{-9}m/s^2$)

	NGF of Satellite 14 pair used as a reference			Difference between 14 and 25			Difference between 14 and 36		
	R	T	N	R	T	N	R	T	N
min	67.212	-41.672	-358.827	-2.096	-0.624	-4.164	-1.321	-0.102	-1.216
max	299.516	24.622	39.400	-0.851	0.892	3.394	1.609	0.178	1.177
mean	176.054	-3.929	-188.744	-1.128	-0.040	-0.454	0.043	0.023	0.004
rms	182.734	12.128	207.835	1.198	0.409	2.196	0.356	0.043	0.318
std	48.958	11.475	87.016	0.403	0.407	2.149	0.354	0.037	0.318

Data analysing

Effects of Drag free control system on velocity interpolation

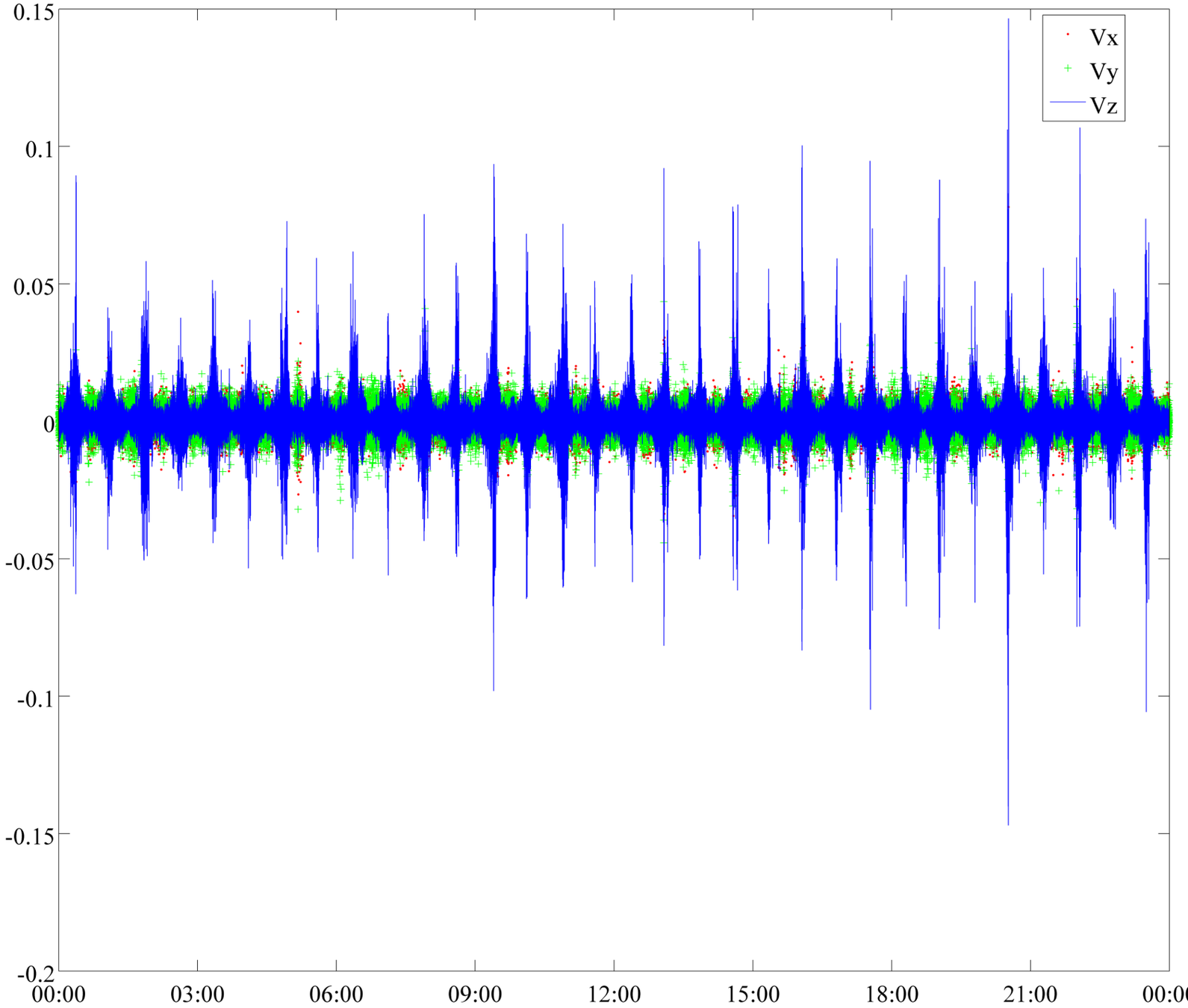

Fig. 7 Difference between the GOCE velocity derived from POD and from the dynamic method (unit: m/s)

Data analysing

Effects of Drag free control system on velocity interpolation

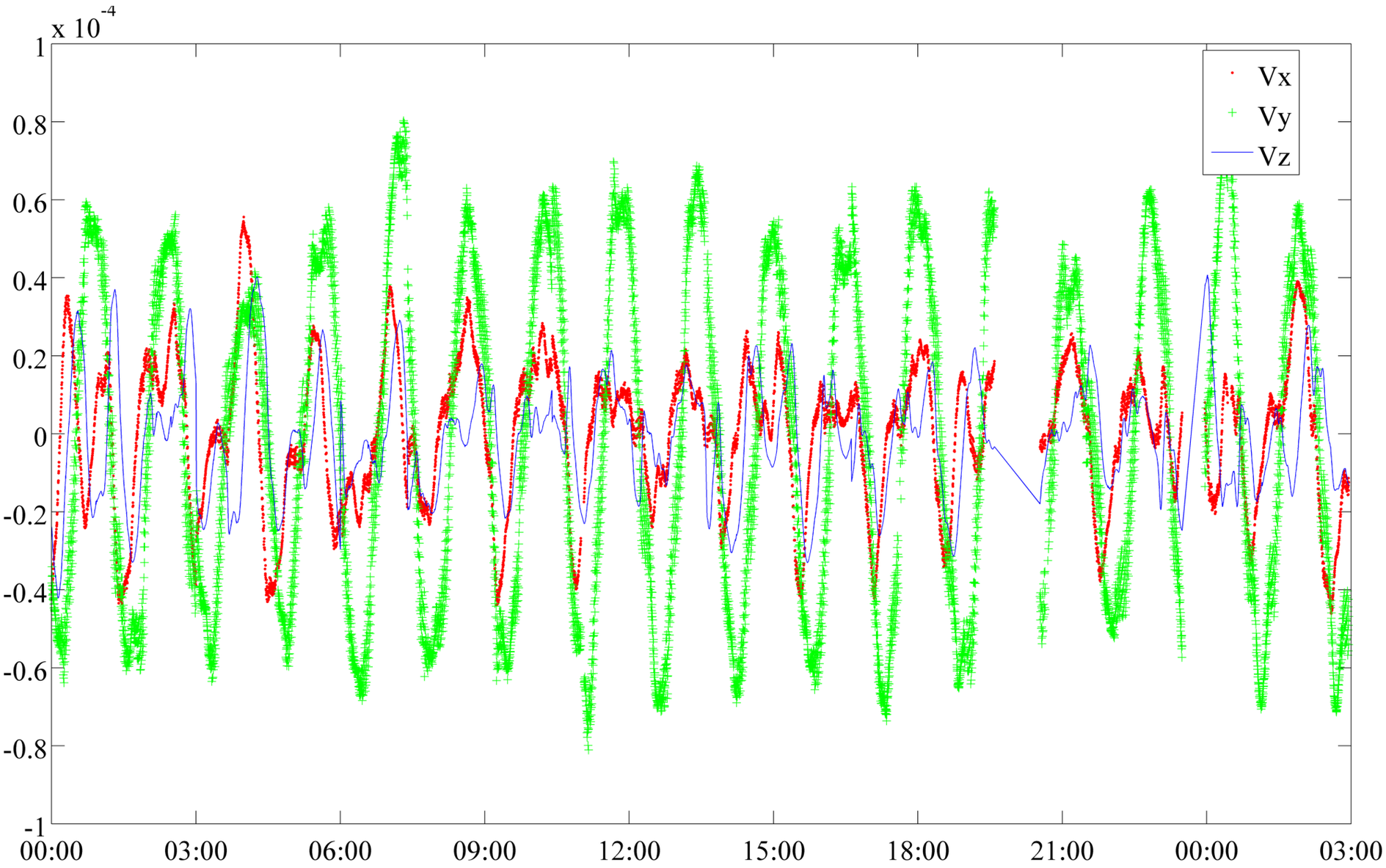

Fig. 8 Difference between the GRACE velocity derived from POD and from the dynamic method (unit: m/s)

Data analysing

Trace of the gravity gradient tensor

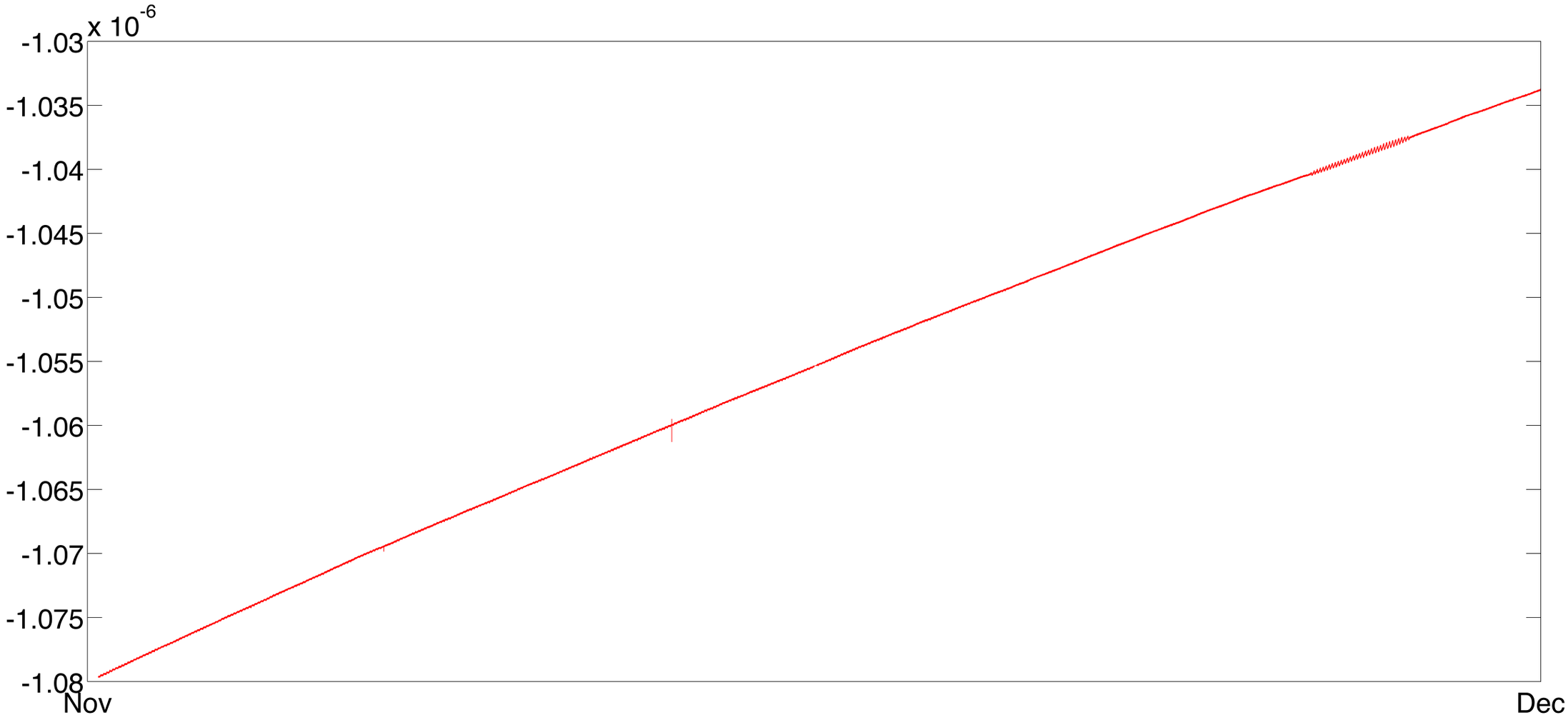

Fig.9 Sum of Vxx,Vyy,Vzz for the GOCE gravity gradients. It is a check of the observables using the Laplace's equation, which shows that there is a clean drift in the GG derived from the original accelerometer readings. (Unit: s^{-2})

Data analysing

Trace of the gravity gradient tensor

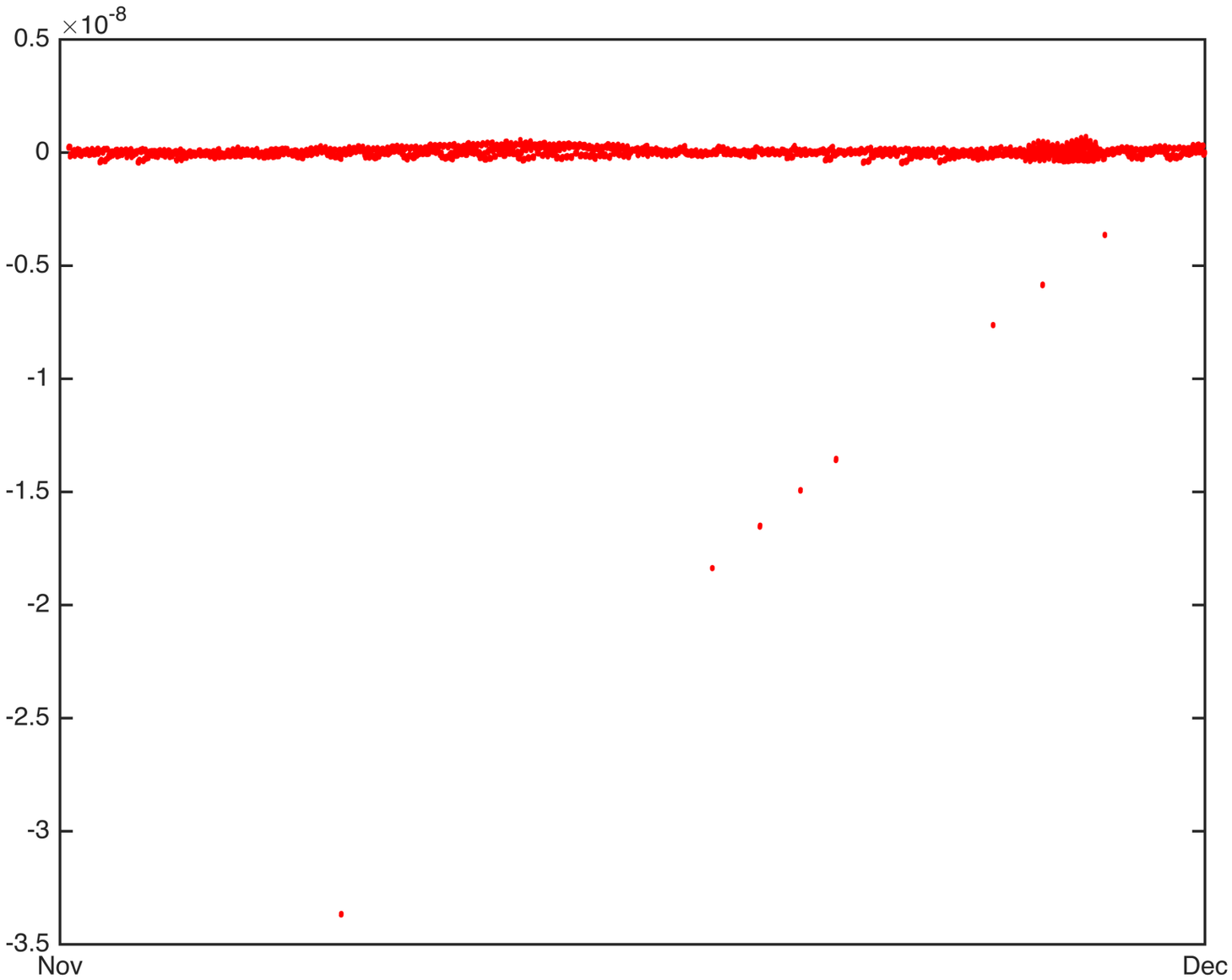

Fig.10 Sum of Vxx,Vyy,Vzz for the GOCE gravity gradients. The drift has disappeared if we use the calibrated data to reconstruct the gravity gradients. (Unit: s^{-2})

Data analysing

Trace of the gravity gradient tensor

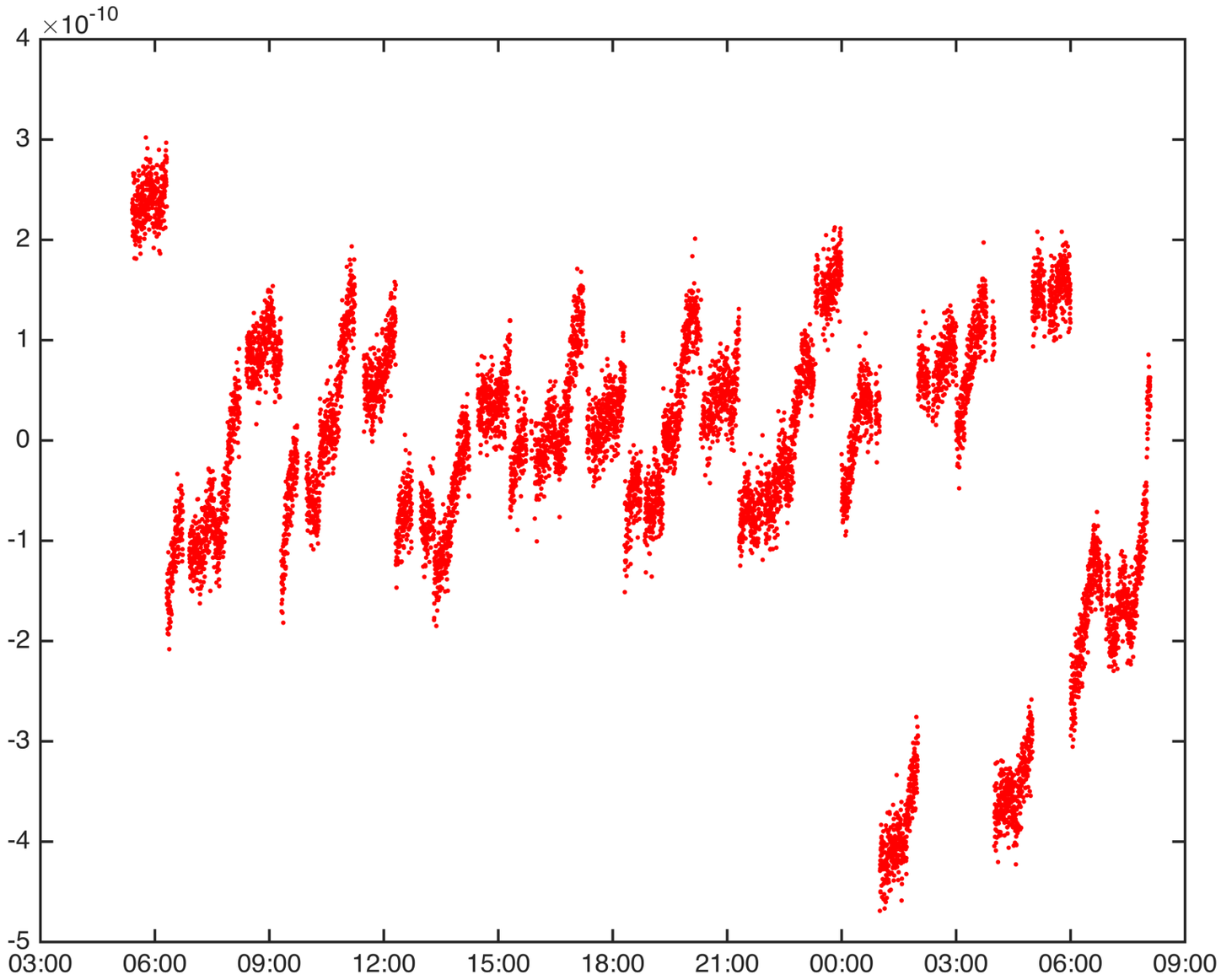

Fig.11 Sum of Vxx,Vyy,Vzz for the GOCE gravity gradients. After the errs are removed from the reconstructed series, the trace of the gravity gradient tensor is several orders of magnitude smaller and close to zero .(Unit: s^{-2})

Data analysing

SHC accuracy distribution (to be continued)

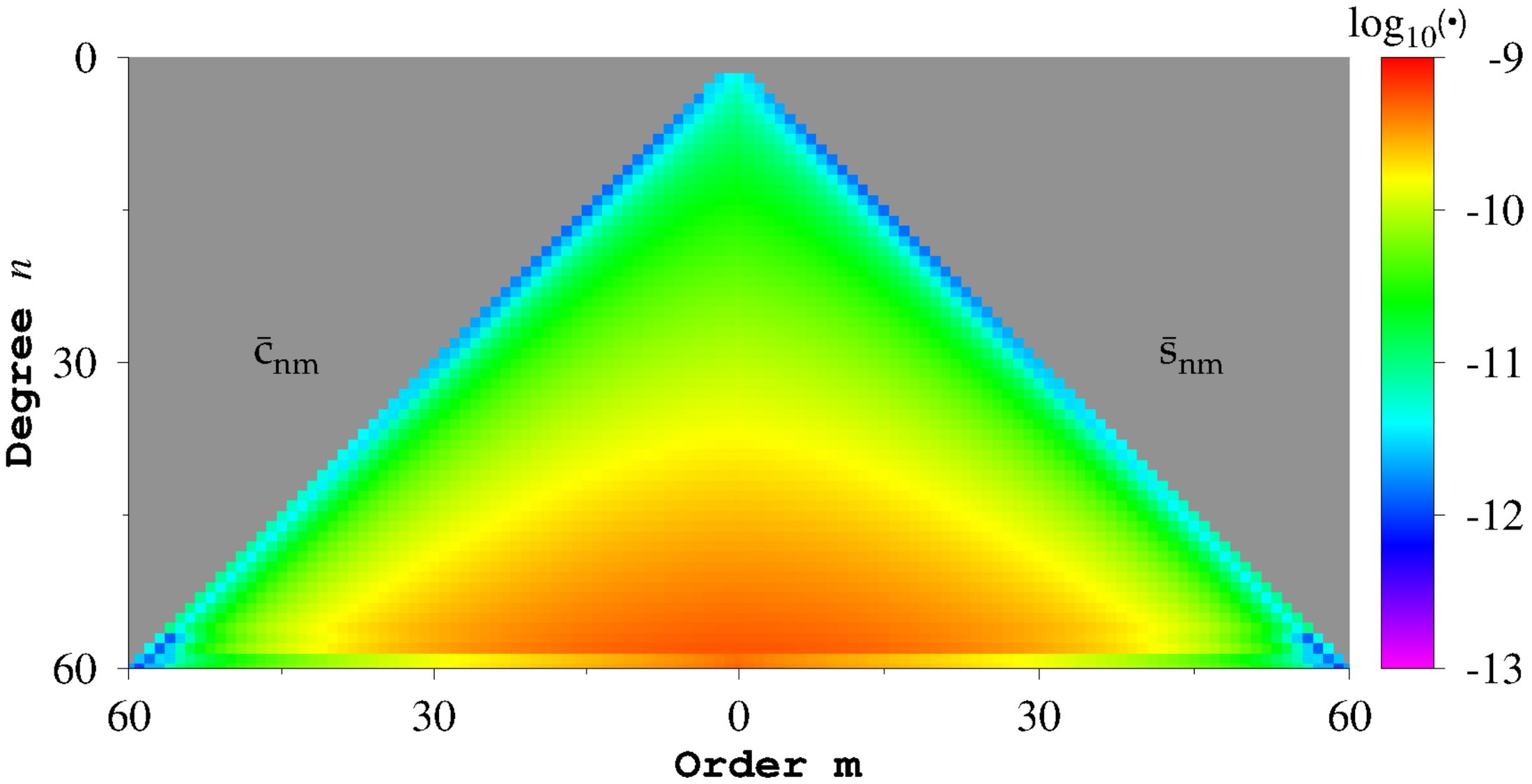

Fig.12 Formal error of the earth gravitational model from the high-low SST data of GOCE only.

Data analysing

SHC accuracy distribution (GOCE v.s. GRACE)

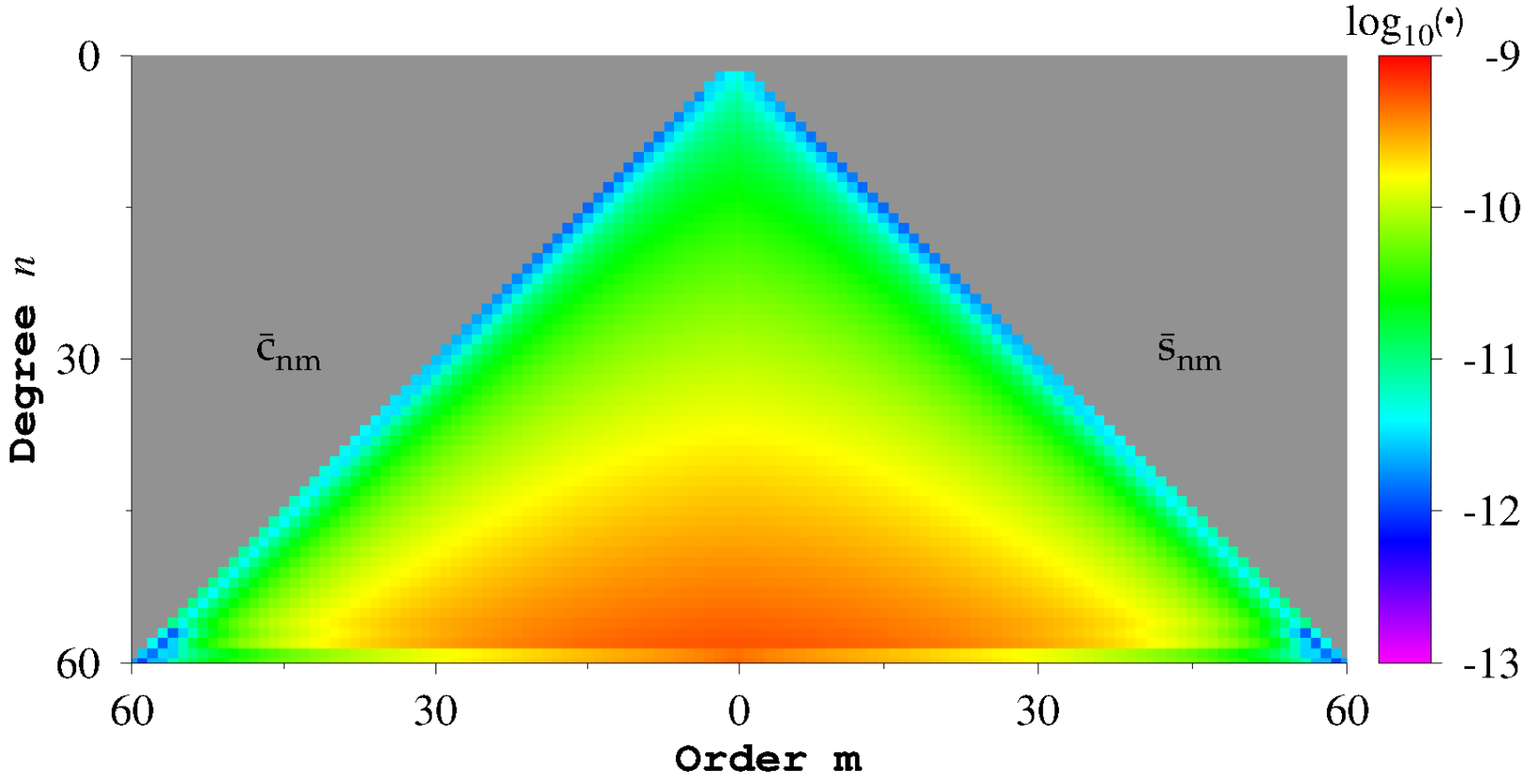

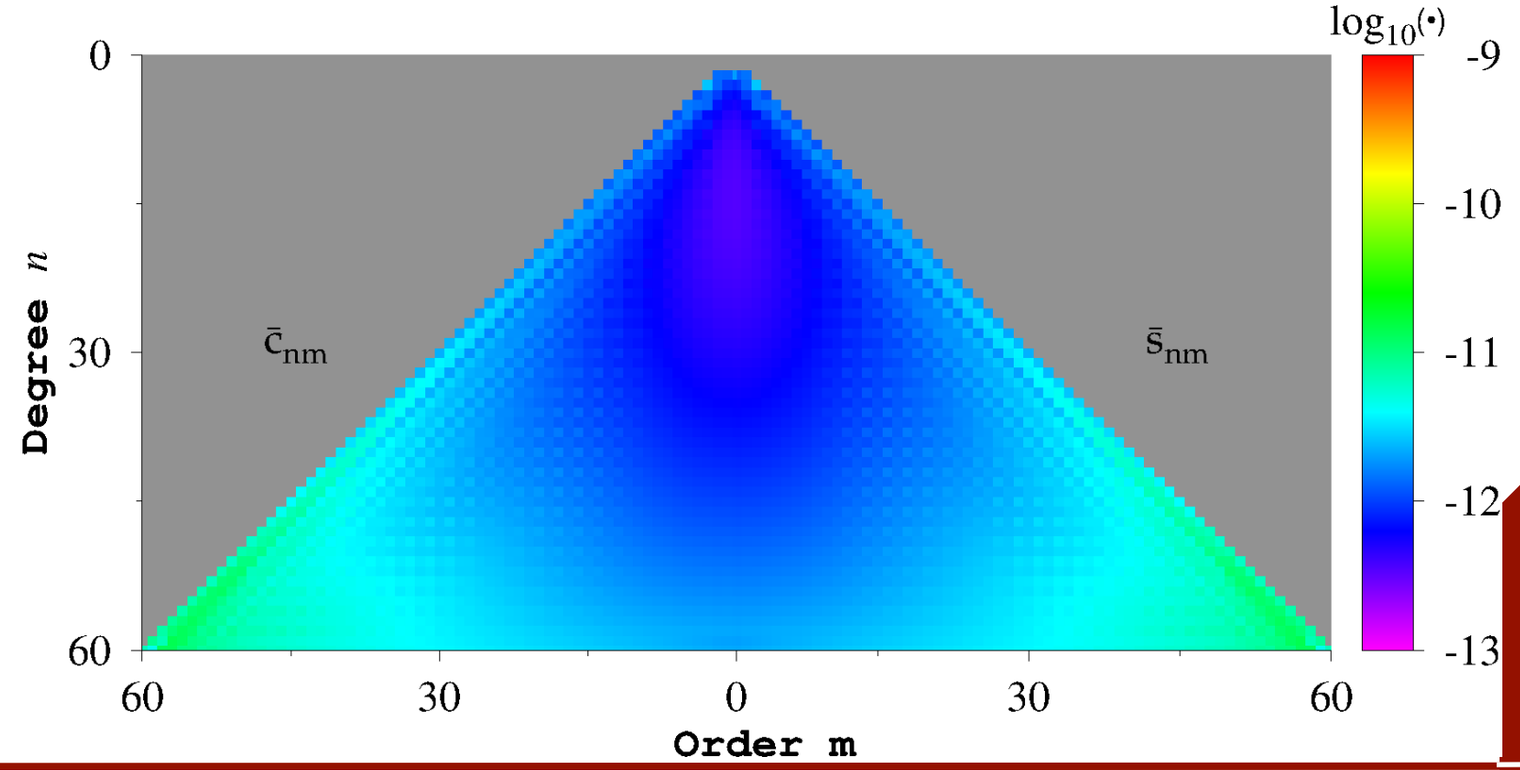

Data analysing

SHC accuracy distribution (GOCE 60x60 v.s. GOCE static solution)

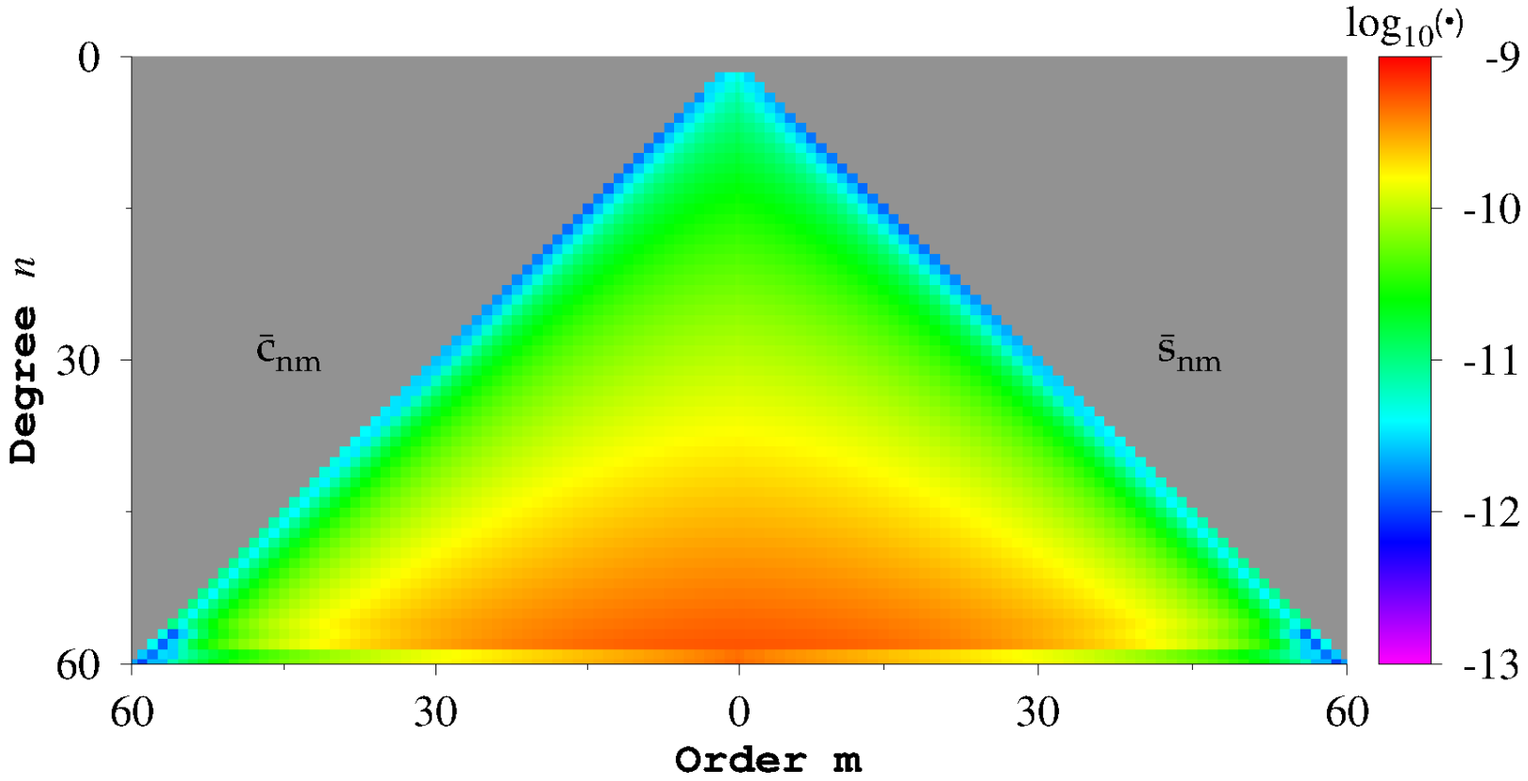

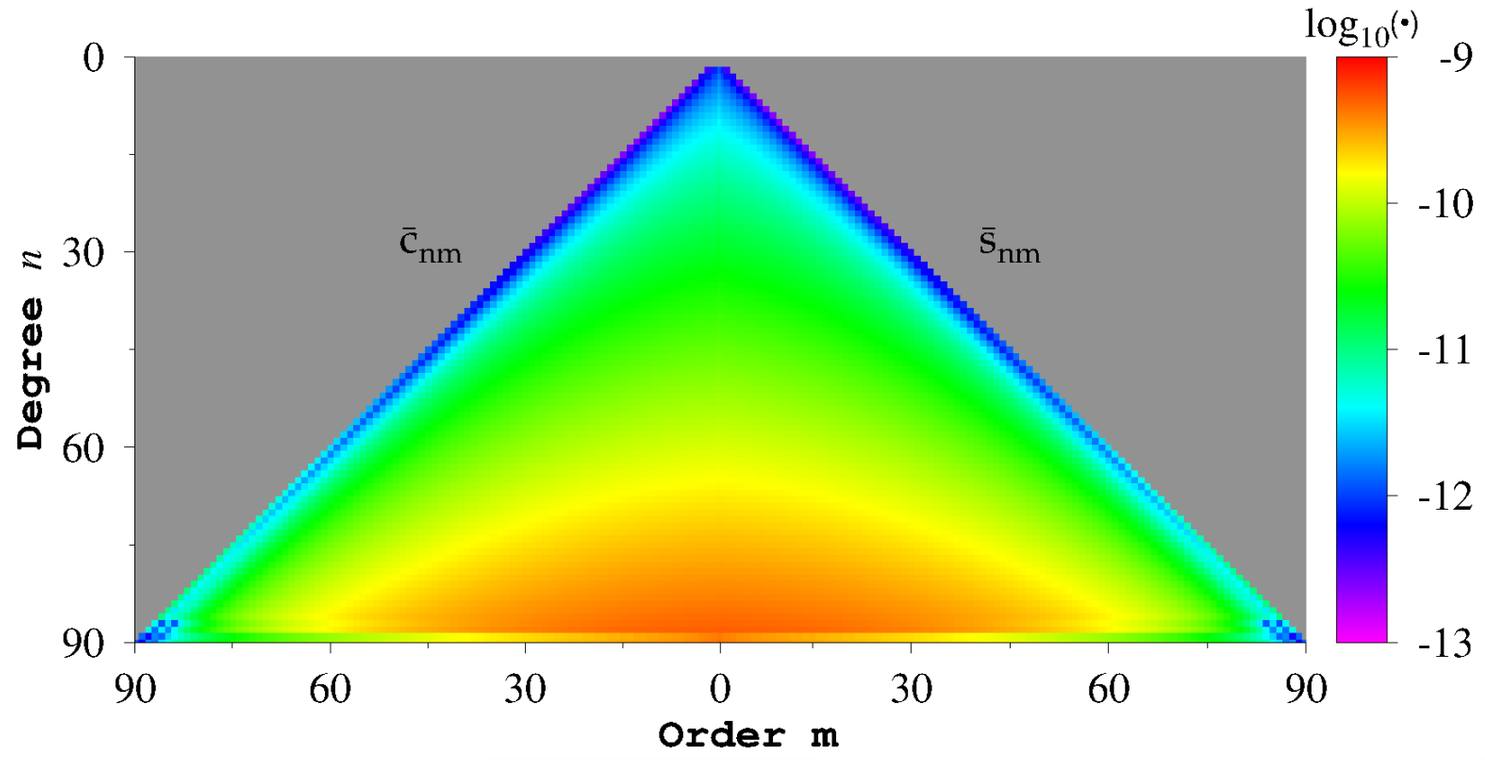

discussions

hl-SST+ll-SST+SGG

- GOCE calibration
  - ✓arm length ?
    - ~51.4,49.9,50.0 cm
  - ✓attitude matrix from 3 cameras
  - ✓a unified model

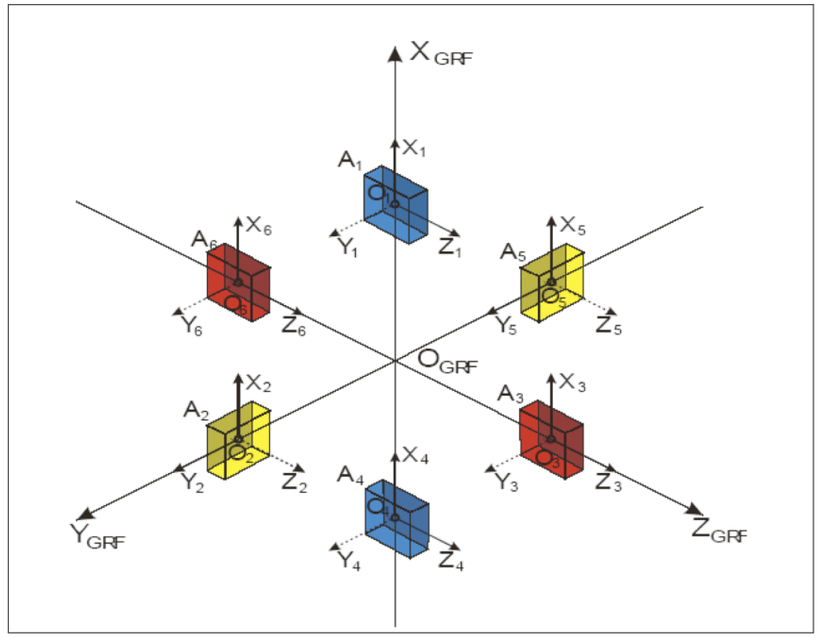

$$\vec{f} = \ddot{\vec{b}} - \nabla V + \vec{\omega} \times \left(\vec{\omega} \times \vec{r} \right) + \frac{d\vec{\omega}}{dt} \times \vec{r}$$

$$\mathbf{r}_{COM} = \mathrm{OI}\left(\mathbf{r}^0_{GRF}, \mathbf{v}^0_{GRF}, \nabla V_0, \mathbf{R}_{GRF \to ECI}, \mathbf{f}_i, \delta\mathbf{f}_i, \mathbf{S}_i, \mathbf{b}_i, \mathbf{r}_i \right)$$

Thanks for your attention

Email: xczou@sgg.whu.edu.cn